DESIGN, FABRICATION AND MEASUREMENTS OF AN S-BAND RADAR IN AN AIRBORNE PLATFORM

A Thesis Presented

by

GERARD RUIZ CARREGAL

Submitted to Universitat Politècnica de Catalunya
Escola Tècnica Superior d'Enginyeria de Telecomunicació de Barcelona
in partial fulfillment of the requirements for the degree of

ENGINYERIA DE TELECOMUNICACIÓ

October 2014

Electrical and Computer Engineering
University of Massachusetts Amherst

DESIGN, FABRICATION AND MEASUREMENTS OF AN S-BAND RADAR IN AN AIRBORNE PLATFORM

A Thesis Presented

by

GERARD RUIZ CARREGAL

Approved as to style and content by:

Paul R. Siqueira, Professor
Electrical and Computer Engineering

To my family

ACKNOWLEDGEMENTS

This work would have been impossible to finish without the help and encouragement of many people.

First, I would like to thank Professor Paul Siqueira, my advisor, for giving me the chance to work on this project. His advice and help have been really important to make this happen.

I would like to thank Dustin for his bright ideas and his help when building the system and testing it. Thanks to Krzysztof because, without his lessons in the workshop and his advice, this radar would have never been tangible. I cannot forget the antennas' guy, thanks Chen for designing them. Thanks Sheila for accompanying me, and the radar, to the hangar. And thank you, Kan and Yang, for your help in the data processing.

Finally, a big thanks to my parents. My little adventure in the U.S. and this thesis would have never happened without their unconditional support, thank you for everything.

ABSTRACT

The need of understanding Earth's complex processes such as earthquakes, volcanoes, ice dynamics or ecosystems requires the design of new instruments. NASA-ISRO Synthetic Aperture Radar (NISAR) is the mission planned to acquire the data that will help the scientific community to conduct this research. One of the instruments of the mission will be an S-band radar.

This thesis describes the process of designing and building an S-band radar, hoping it will help, in the following years, in the study of what kind of results can be obtained at this frequency band. The thesis reviews all the process needed to build the radar and test it, explaining how it was installed in an aircraft to take measurements and showing the first results obtained.

TABLE OF CONTENTS

LIST OF TABLES

LIST OF FIGURES

CHAPTER 1

Introduction and Motivation

1.1 NISAR mission

NASA-ISRO Synthetic Aperture Radar (NISAR) is a joint mission between Nation Aeronautics and Space Administration (NASA) and Indian Space Research Organization (ISRO). The mission will launch a satellite equipped with two Synthetic Aperture Radar (SAR) working at L-band and S-band. The satellite is likely to be launched in 2020.

Interferometric and polarimetric measurements using two different wavelengths will generate a very valuable dataset not often acquired. Moreover, NISAR will provide an unprecedented coverage in space and time that will be decisive in the study of ecosystem disturbances or natural hazards. [4]

NISAR scientific goal is to study and understand some of the Earth's most complex processes. The obtained data will help the scientific community to study ecosystems (biomass, effects of changing climate on habitats and CO2, agriculture), ice dynamics (ice velocity and thickness, response of ice sheets to climate change and sea level rise) and solid earth geophysics (surface deformation, hazards response and water resource management). The research in these fields will improve, for instance, disaster forecasting (earthquakes, volcanoes, floods...) or the understanding of how the climate change affects the carbon cycle. [3]

1.2 Motivation

The S-band radar developed at the Microwave Remote Sensing Laboratory (MIRSL) will provide data to study the behavior and response of vegetation and water at the S-band wavelength. This research, the characterization of some electromagnetic properties of biomass and

water, may help in future stages of the NISAR mission.

The development of the S-band radar presented in this thesis seeks to provide an initial version of a working radar. Furthermore, it identifies the main issues of the system and finds possible solutions. This work is just the first step on a project that should keep going on to achieve attractive results. Hopefully, it will be useful in future designs of the S-band radar as well as to help study the response of natural targets (radar cross-section, polarimetric, interferometric and otherwise) to this frequency band.

CHAPTER 2

Radar Concepts

The word radar stands for Radio Detection And Ranging. As its name indicates, a radar uses electromagnetic pulses to detect and position targets. The basic operation consist of sending a short energetic pulse and measuring the time it needs to come back. Thus, the distance travelled by the pulse can be calculated using

$$t = \frac{2r}{c}. \tag{2.1}$$

In FMCW radar, the duty cycle of the pulse is 100%, that means that transmitting and receiving are performed simultaneously. The pulse used is a chirp pulse, a sinusoid changing its frequency with time. The advantage of using a chirp is having an energetic pulse with a wide bandwidth.

The chirp used in the S-band radar is linear with slope $\frac{B}{\tau}$, the equation describing the frequency variation is

$$\Delta f = \frac{B}{\tau}\Delta t. \tag{2.2}$$

Instead of calculating the time the pulse has travelled, a mixing operation (product of the frequencies) is used to find out the range the pulse has travelled. The two mixing signals will be: the pulse before transmission and the received pulse. The mixing operation will result in the difference and the sum of the input frequencies. The difference is called the beat frequency and it is proportional to the range travelled by the pulse. The equation is

$$f_b = \frac{B}{\tau} \cdot \frac{2r}{c}. \tag{2.3}$$

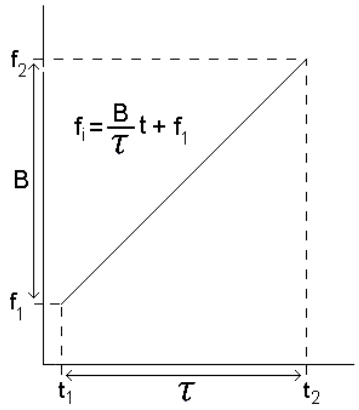

Figure 2.1: Chirp slope.

From the equation it is deduced there are $f_{max} \cdot \tau$ range bins, and each range bin is equal to $\frac{c}{2B}$. Therefore, the range resolution of the radar is $\frac{c}{2B}$.

Another interesting parameter is the gain compression, which results from the hardware compression of the chirp pulse. The gain compression is given by the equation

$$G_c = B\tau \tag{2.4}$$

and is the factor the SNR is increased after the compression.

CHAPTER 3

System Design

3.1 System overview

The radar system is composed of the radar transceiver, with a transmit antenna and two receivers; a signal generator, the power supply, that includes a GPS receiver and a 10 MHz local oscillator and the acquisition computer. The block diagram of the system is shown in Figure 3.1.

The signal generator generates a chirp pulse continuously. Every time a new pulse is generated, a TTL rising pulse (trigger) is sent to the Analog to Digital Converter (ADC) card. Once the chirp signal is generated, it enters into the transceiver. The transceiver also gets a 10 MHz reference signal that is used to phase lock the local oscillators. The chirp signal coming from the signal generator is split. One of the split signals travels through the up-converter and it is transmitted. The other is used as oscillator in the signal compression stage. The echo is received in both receive antennas and it is down-converted. The signal compression stage is applied to both receive channels to perform chirp compression in real time. Finally, the ADC will sample the signal of the receive channels. The acquisition software that controls the ADC is LabVIEW. The code plots the data while it is written onto a file. The data is processed afterwards in the lab using MATLAB. The received data from channel 0 (CH0) and channel 1 (CH1) can be used to get interferometric measurements.

Since TIMMi's (Topographic Ice Mapping Mission) setup in the aircraft [5] worked well, the S-Band system has been designed to be as close as possible to TIMMi's setup. Thus, the power supply is TIMMi's power supply slightly modified. The signal source is the Tektronix AFG3252. The acquisition computer is the NI PXIe-1062Q with the NI PXI-5152 8-bit 2 GS/s digitizer. The six-patch array that makes up each antenna (Figure 3.3) was designed by Xingjian Chen, a master's student at MIRSL, and mounted in the aircraft door (Figure 3.4).

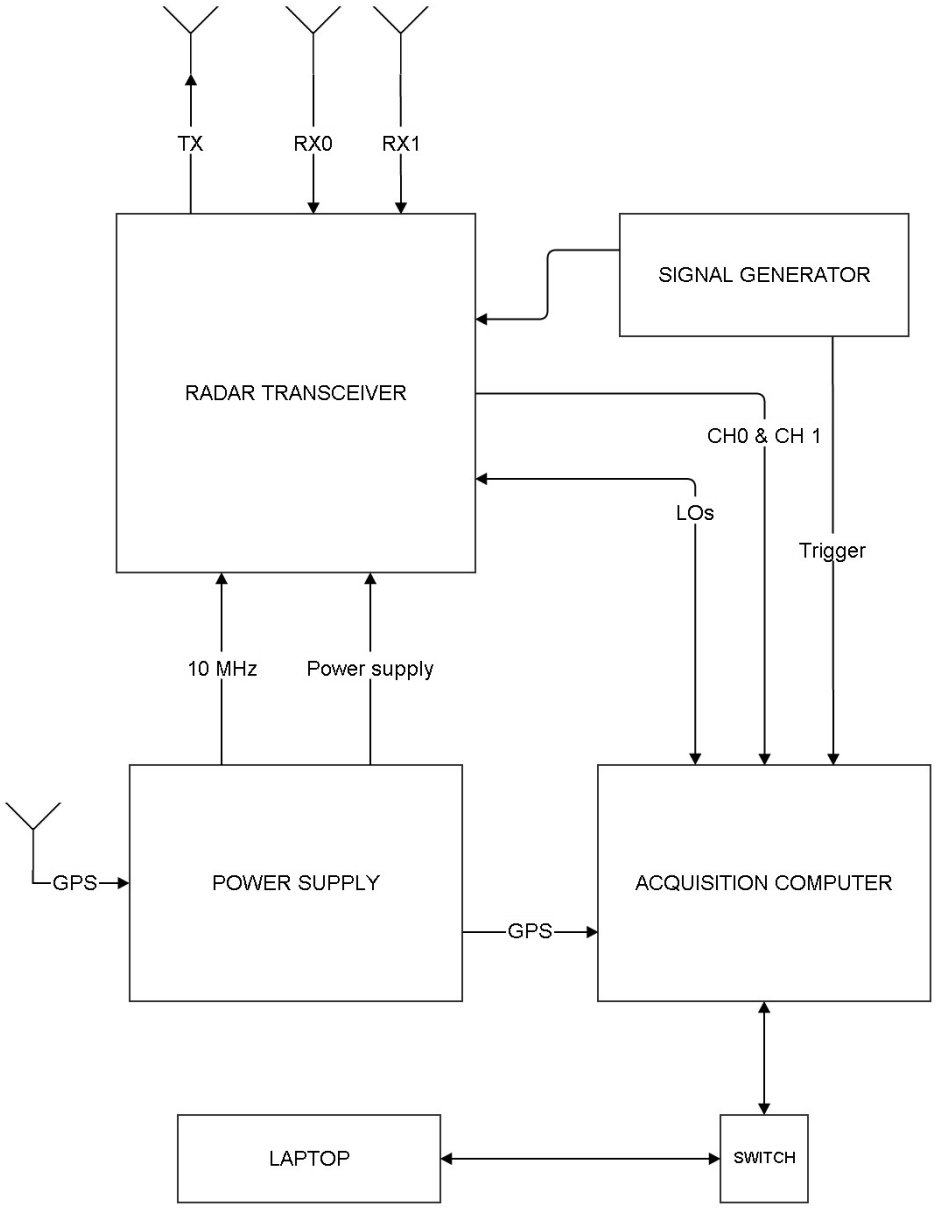

Figure 3.1: Block diagram of the radar system.

3.2 Power supply

The power supply used for the system is the TIMMi's power supply with some minor modifications. The existing power supply enclosure had a 15 V Vicor power supply, a 9 V regulator, a GPS and a local oscillator of 10 MHz. A 5 V Acopian and a 28 V/15 V Vicor power supplies were added to the existing box. Moreover, the 9 V regulator was changed and a 12 V regulator was installed instead. Some elements had to be rearranged to get free space to add the new power supplies. The 28 V/15 V power supply had to be mounted upside down to fit in the box. Figure 3.2 shows the new setup inside the power supply box.

The pinout of the circular military connector had to be modified, new pins were added. Table 3.1 lists the new and old pinouts.

The GPS receiver is connected via USB to the acquisition computer. It has an SMA connector for the antenna. There is a GPS SMA antenna to run tests in ground measurements. In the airplane, it is connected to one of the airplane antennas. The GPS data is used to save a timestamp on each measurement done while flying. Thus, the RF data can be merged with the motion data of the airplane.

3.3 Acquisition computer

In order to use TIMMi's acquisition software, the NI PXIe-1062Q was used in all the measurements with the NI PXI-5152 8-bit 2 GS/s digitizer. In FMCW radars, the sample frequency is usually low. In the radar presented in this thesis, was never higher than 10 MHz. The NI PXI-5152 digitizer is capable of sampling at much higher frequencies. Therefore, the restriction in the maximum frequency that can be sampled is given by the write speed of the hard disk. In the last measurements, the maximum sample frequency that could be used by both channels was 6 MHz. The solid state drive of the computer had to be changed before the first flight since it stopped working. TIMMi's original HDD was cloned to the new 128 GB SSD.

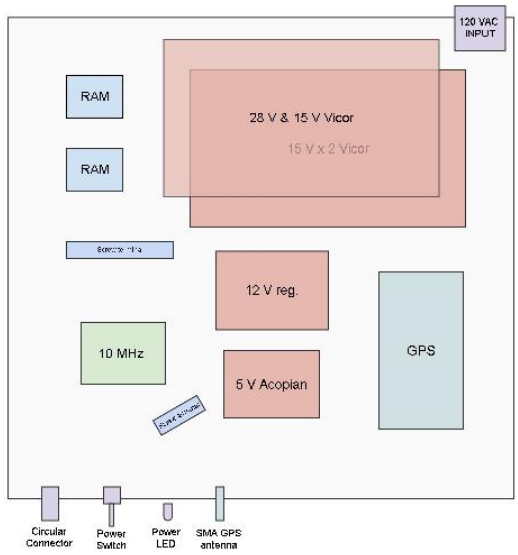

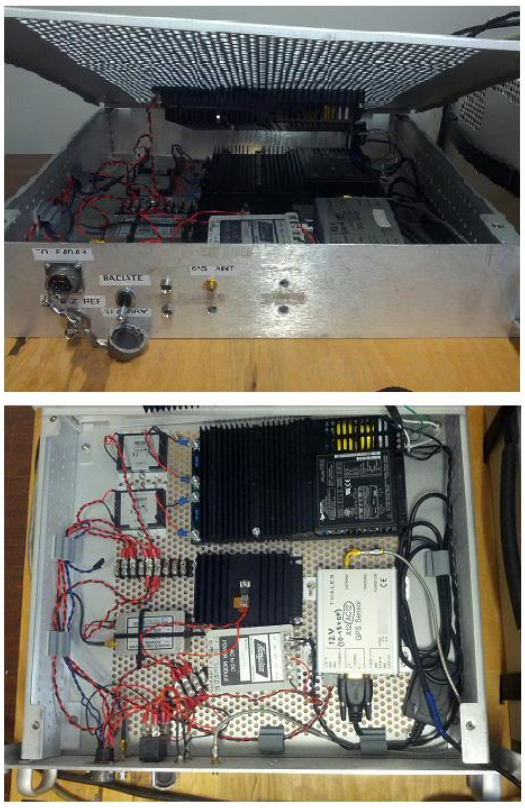

Figure 3.2: Layout of the modified power supply enclosure.

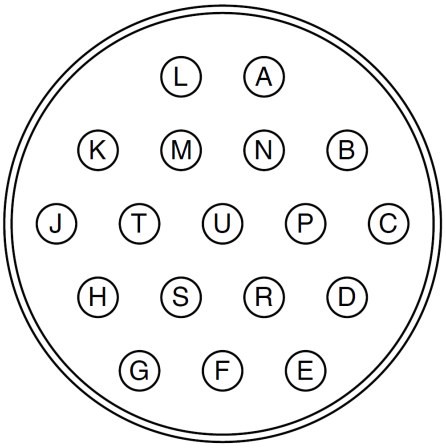

Pin	S-band radar		Ka-band airborne radar	
	V	Use	V	Use
A	+15	BB & Tx amps.	+15	LOs, BB amps.
B	GND	BB & Tx amps.	GND	DUC & DDC
C	+15*	Not used	+15*	DUC & DDC
D				
E				
F				
G	+5*	LNA, LOs amps.		
H	GND	LNA, LOs amps.		
J	+12	Rx L-band amp.	+9	Power amp.
K	GND	Rx L-band amp.	GND	Power amp.
L	GND	Not used	GND	LOs, BB amp.
M	GND	HPA		
N	+28*	HPA		
P				
R				
S				
T				
U				

Table 3.1: **Power supply 18-pin circular connector for S-band radar and Ka-band airborne radar. The voltages marked with an asterisk (*) are always on during standby. Blank entries are not connected.**

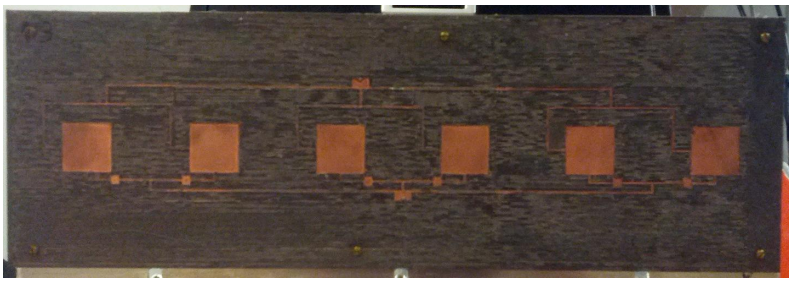

Figure 3.3: One of the antennas used in the flight measurements.

3.4 Antennas

The system uses three antennas. One for the transmitter and two for the receivers. The antennas were designed and built by Xingjian Chen, a master's student at MIRSL. They were built using a milling machine in a substrate made by a company named Rogers Corporation. Because of the building process, their response is not exactly the same even if the same design was used.

The design is a six-patch array antenna with vertical and horizontal polarizations. The center frequency is 3.2 GHz and the bandwidth 100 MHz. In the measurements presented in this thesis, vertical polarization was used. In the vertical polarization, the azimuth beamwidth θ_H is 12 degrees (0.21 rad); the elevation beamwidth θ_V is 60 degrees; the gain in the main lobe is 12 dB; and the difference between the main lobe gain and the side lobe gain, the Side Lobe Level (SLL) is 10 dB.

In the simulations, the transmit antenna has the center frequency slightly shifted compared to the receive antennas. However, the ground measurements revealed that it was not a big issue, and the center frequency of the transmitted chirp did not need a change. The two polarizations have some differences, especially in the beamwidth of the antenna main-lobe in the azimuth and elevation directions.

3.5 Aircraft door modifications

The aircraft door had to be modified to mount the new antennas. The old structure was removed. The easiest solution to mount the antennas without spending too much time was to mount them in a fixed angle of 45 degrees as we can see in Figure 3.4. The distance between

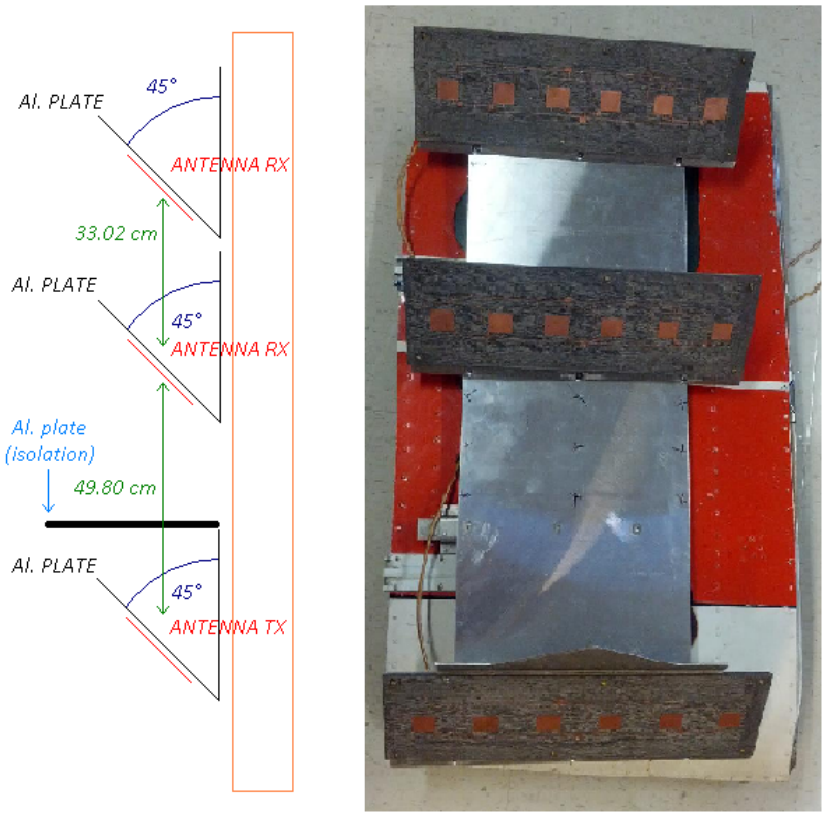

Figure 3.4: Sketch of the disposition of the antennas in the door and picture of the built structure.

the antennas was decided taking the dimensions of the door and the response of the antennas into account . Since the main challenge was to weaken the near field coupling between the transmitter and the receivers, the distance between them is maximized.

All the modifications were made by Thomas Liimatainen, a machinist at Mount Holyoke College.

3.6 Radar transceiver overview

The radar uses two stages to convert the signal from base band to S-band. There are two reasons to use this design: image rejection improvement and the possibility to use an already existing L-Band PCB design in the future. Therefore, the radar has two up-conversion and two down-conversion stages. Moreover, since the radar will be used as FMCW, there is the

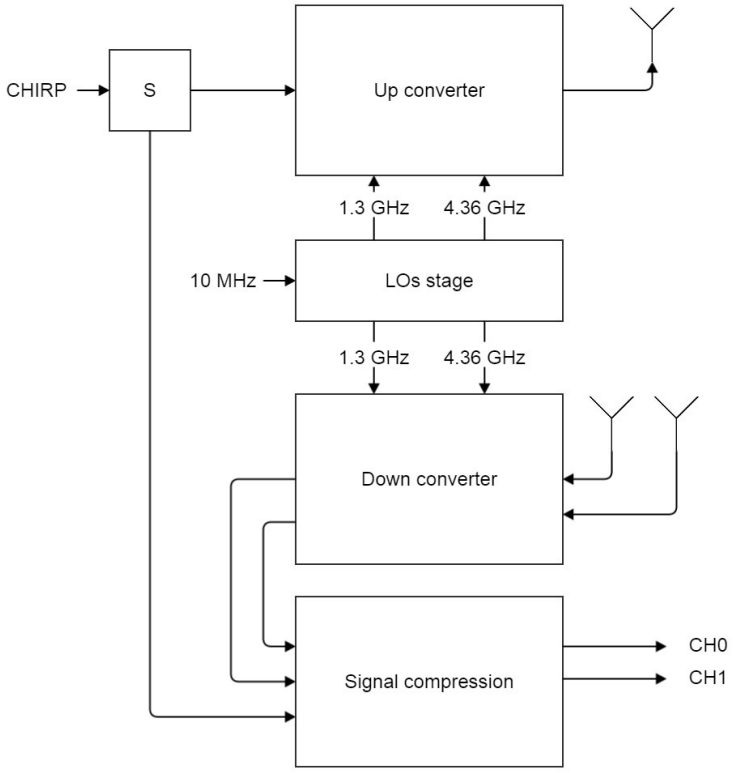

Figure 3.5: Block diagram of the transceiver of the radar.

signal compression stage. An LOs stage is also needed to make the different stages work. The block diagram is shown in Figure 3.5. The actual radar has two down-converters and two signal compression stages, one for each receive antenna. The phase of the signal received is important to generate interferometric images. The receivers should be as symmetric as possible to avoid different phase changes on each receiver.

The mixer operations in the up-converter produce the sum and the difference of the two input and LO frequencies. Hence, there will be an upper side band (sum) and a lower side band (difference). In the system, the lower side band is used in both up-conversions. In the down-converter, the mixing operations can result in false target detection if there is a strong signal in the image frequency band. The down-converter must be robust to the three image frequency bands that can be seen in Figure 3.6. The frequency specifications of the radar are listed in Table 3.2.

Parameter	Value
Siganl bandwidth	200 MHz
S-band center frequency	3.2 GHz
L-band center frequency	1.16 GHz
Base band center frequency	140 MHz
S-band LO frequency	4.36 GHz
L-band LO frequency	1.3 GHz

Table 3.2: Frequency specifications of the radar.

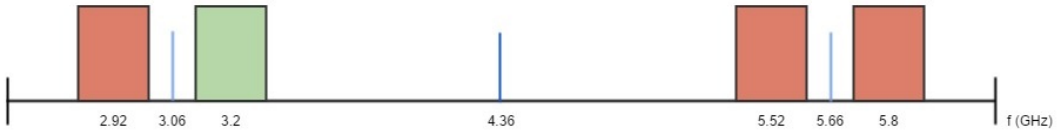

Figure 3.6: Spectrum with the three image frequency bands, in red; the local oscillators, in blue; and the working band of the radar, in green.

3.7 Up-converter

Once the base band signal enters into this stage, the goal is to shift it up in frequency. To do so, the signal will go through two sub-stages. The first will up-convert the signal from base band to the L-band. The second will up-convert it from L-band to S-band.

Figure 3.7 shows the block diagram of the up-converter.

Each sub stage of the up-converter is made of a mixer that shifts up in frequency the signal and a filter whose goal is to attenuate the image frequency band. Once the center frequency

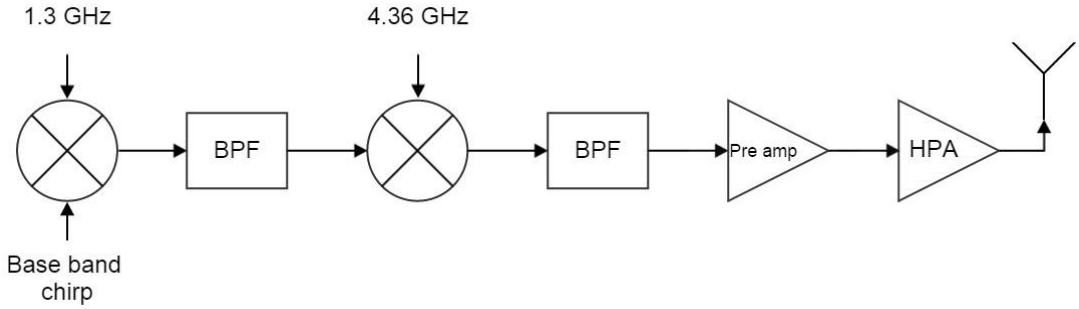

Figure 3.7: Block diagram of the up-converter.

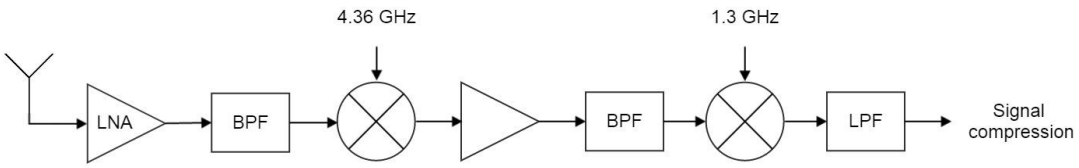

Figure 3.8: Block diagram of the down-converter.

is 3.2 GHz, the signal must gain power before being transmitted by the antenna. The system uses a High Power Amplifier (HPA) before the signal is transmitted.

3.8 Down-converter

When the signal is received, the down-converter will shift it back to the base band. The received signal will encounter a Low Noise Amplifier (LNA) immediately after the antenna. The LNA is essential to have a good Noise Figure (NF), using an amplifier with a higher NF would reduce our sensibility to detect weak signals. The LNA will be followed by a set of filters, mixers and an amplifier as shown in Figure 3.8. These components will be responsible for bringing the signal back to base band while increasing its power.

The image frequency rejection is an important goal the down-converter must achieve. The filters will be responsible for attenuating the image frequency band as much as possible. When choosing the filters, a trade off between a high rejection and a good phase linearity of the signal must be done. For instance, if a filter with a very sharp response is chosen, it will reject the image frequency band but its phase will be nonlinear.

3.9 Signal compression

Since the radar is used as an FMCW radar, a signal compression stage was designed. The signal compression gets the beat frequency and amplifies the signal before it is sampled by the ADC. It has a mixer, which gets the beat frequency; a filter, responsible of reducing the noise bandwidth and rejecting unwanted signals resulting from the mix operation; and an amplification stage.

The block diagram is shown in Figure 3.9.

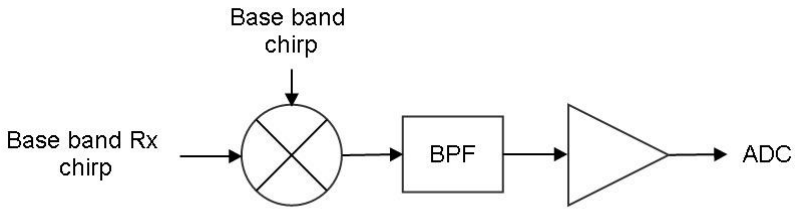

Figure 3.9: Block diagram of the signal compression stage.

The filter is a bandpass filter composed of a high pass and a low pass filter. The high pass filter rejects the low frequencies containing unwanted high power signals coming from the near field coupling between antennas. Initially, a DC-block was used. Since the coupling was still very strong, a high pass filter made in the lab was added. The low pass filter limits the bandwidth of the spectrum to sample, reducing the noise bandwidth integrated and avoiding aliasing. If Nyquist sampling theorem is not satisfied, aliasing can be observed and will result in false target detection.

3.10 Receiver specifications

The down-converter and the signal compression form the receiver of the radar. There are some interesting definitions and calculations that can predict the behavior the receiver will have when a signal comes in. Since these calculations are made for ideal systems where effects like coupling through the ground plane are not included, the results must be taken cautiously.

- Nose Figure (NF). The NF of a system measures de degradation of the Signal to Noise Ratio (SNR) in the system[1]. It compares the output SNR of the system to the SNR in the input. The signal and the noise are attenuated or amplified through the receiver at the same rate. Moreover, each component adds some noise resulting in the increasing of noise power in the system. Therefore, the output SNR is lower than the input SNR. The equation describing the NF is

$$NF = NF_1 + \frac{NF_2 - 1}{G_1} + \frac{NF_3 - 1}{G_1 \cdot G_2} + \cdots + \frac{NF_n - 1}{G_1 \cdots G_{n-1}}. \tag{3.1}$$

  Notice that the second term of the equation is attenuated by the gain of the first component.

The third is attenuated by the gain of the first component and the second component and so on... The first component is decisive in the system's NF. This is why an LNA needs to be the first component in the receiver, it will amplify the signal while only slightly worsening the NF. The calculated NF of the S-band receiver is 1.54 dB.

- Third-Order Intercept Point. Due to nonlinearities, active components such as amplifiers or mixers, generate spurious frequency components. The third order intermodulation products are specially important since they are close to the desired working band. The Third Order Intercept Point is defined as the point where the first-order and third-order frequency components have the same power [1]. At this point, the system has a nonlinear behavior. The intercept point for a cascaded system is defined by the equation

$$\frac{1}{IP_3} = \frac{1}{IP_{3_n}} + \frac{1}{IP_{3_{n-1}} \cdot G_n} + \cdots + \frac{1}{IP_{3_1} \cdot G_n \cdots G_2}. \tag{3.2}$$

  The calculated IP3 of the S-band receiver is 16.91 dBm (at the output).

- Dynamic Range (DR). The operating range where the system is working in linear conditions is defined as the Dynamic Range [1]. The DR is limited at the low end by noise and at the high end by the compression point (DR_l) or the maximum power level where the intermodulation products are not acceptable(DR_f). Here it is presented how to calculate the DR_f,

$$DR_f(dB) = \frac{2}{3} \cdot (IP_3 - N_o). \tag{3.3}$$

  To calculate any of the DR, it is necessary to know the noise power (N_o) at the receiver output, which is defined by the equation

$$N_o = G \cdot k \cdot B \cdot [T_a + (NF - 1) \cdot T_0]. \tag{3.4}$$

  The parameters of the receiver are: Gain (G) = 60 dB, Bandwidth (B) = 2.5 MHz and NF = 1.54 dB. The Boltzmann constant is k = $1.38 \cdot 10^{-23}$ and T_0 = 290 K. Moreover, a T_a = 150 K will be assumed. Thus, N_o = -50.25 dBm.
  The resulting DR_f of the S-band receiver is 44.8 dB.

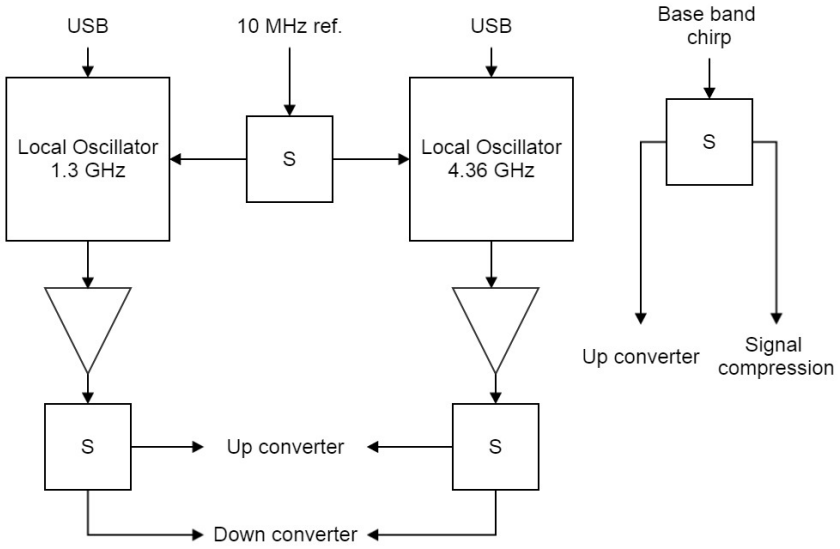

Figure 3.10: Block diagram of the local oscilators stage.

It is important to remember that these results are approximated, the values just give an idea of what to expect.

3.11 Local Oscillators (LO) stage

The mixers working in the transceiver need three oscillators. First, the L-band mixers need the LO working at 1.3 GHz. Second, the S-band mixers work with a 4.36 GHz oscillator. And last, the signal compression mixers need the chirp pulse, before it is sent to the up-converter, as an oscillator. The LOs are phase-locked by a 10 MHz sinusoid signal provided externally. Therefore, this stage is composed of the S-band and L-band local oscillators, the chirp pulse, a bunch of splitters to send the LOs and the chirp to the transceiver and some amplifiers to adjust the power of the signals. In Figure 3.10 the block diagram of this stage is shown.

CHAPTER 4

Building the radar

This section describes briefly how the system was built in its latest version. It also gives information of each component used to build it.

4.1 Enclosure

The distribution of the different stages in the enclosure is shown in Figure 4.1 and Figure 4.2. Since the space is limited inside the airplane, the enclosure was chosen to be as small as possible. Therefore, the distribution of the elements inside the enclosure is tricky and not always optimal when the electromagnetic environment is taken into account. The up-converter, down-converter and signal compression stages are all together in one side of the enclosure at different levels. The LOs stage is in the middle of the enclosure. The HPA is on the other side. Initially, the HPA was supposed to be mounted also in the up-converter level to avoid crossing wires going from one side of the enclosure to the other one with high power signals. It was not possible to get the initially selected HPA. The new one had to be placed on the other side because of the size of its fan. The power distribution is divided in two sections. Each of the amplifiers has two capacitors between the DC-GND terminals. The capacitors act as a low pass filter, trying to attenuate all the AC signals. Furthermore, if the amplifier draws a high peak of current, the capacitors will help weakening this effect.

The system is built using SMA components. S-band is a relatively low frequency, and hence the components are generally available. For this system, most of the components were acquired from a company named MiniCircuits.

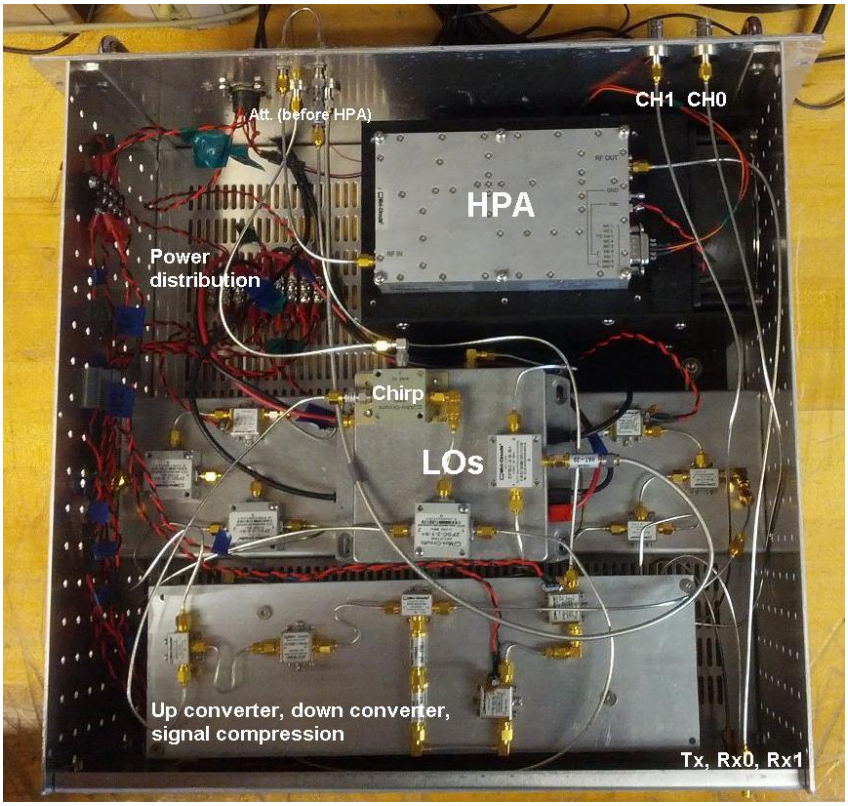

Figure 4.1: Top view of the radar enclosure.

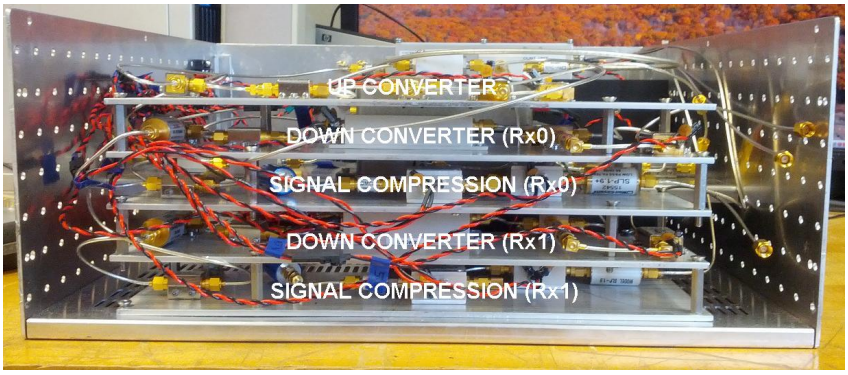

Figure 4.2: Side view of the radar enclosure.

Reference (MiniCircuits)	Component type	Specifications	Use
ZX05-43LH+	Mixer	LO Power +10dBm, Conversion Loss 6.3dB	Up-conversion to L-band
ZX75BP-1100+	Band Pass Filter	Fast roll-off on the upper side band, Passband = 1000-1200 MHz	LO and image frequency band attenuation
ZX05-83LH+	Mixer	LO Power +10dBm, Conversion Loss 5.6dB	Up-conversion to S-band
VLF-3000+	Low Pass Filter	Passband = DC-3600 MHz	Attenuate image frequency band
VHF-2700+	High Pass Filter	Passband=2500-6500 MHz	Clean lower side spectrum
ZX60-4016E+	Amplifier	Gain 16dB, P_1=16dBm, IP_3=28dBm	Amplify the chirp pulse before the HPA
ZHL-16W-43+	High Power amplifier	Gain 45 dB, P_1=42.5dBm, IP_3=48.5dBm	Amplification before transmit antenna

Table 4.1: Components used in building the up-converter. All of them have SMA connectors.

4.2 Up-converter

The up-converter was built with the components listed in Table 4.1. Moreover, some attenuators are used before the HPA to avoid its saturation.

The mixers were chosen because of their frequency range and price. The L-band filter used has a very high roll-off in the high frequency stop band which is important to attenuate the image frequency band, which is very close to the radar's band. Since there were no S-band bandpass filters that met the requirements the system needs, a low pass filter and a high pass filter are mounted in cascade. The S-band amplifiers and the attenuators are used to amplify the pulse to get the maximum possible power at the antenna. If the power needs to be decreased, the enclosure has two external SMA connectors where more attenuators can be connected. Thus, this little stage can be used to add attenuation before the pulse goes into the HPA. The HPA has a maximum output of 16 W. The high power helps to be able to detect weaker signals but it also worsen the coupling between antennas and the saturation of the system.

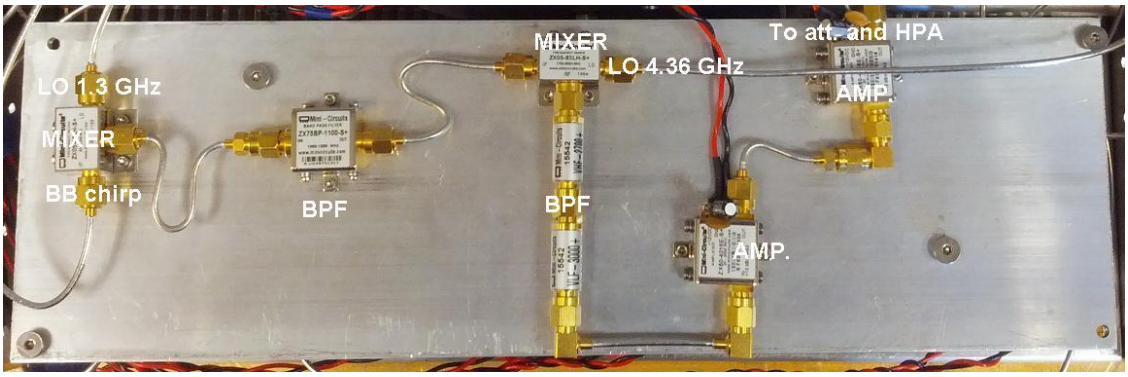

Figure 4.3: **Up-converter. The BB chirp is up-converted (travels from the left to the right) and it is ready to be amplified in the HPA.**

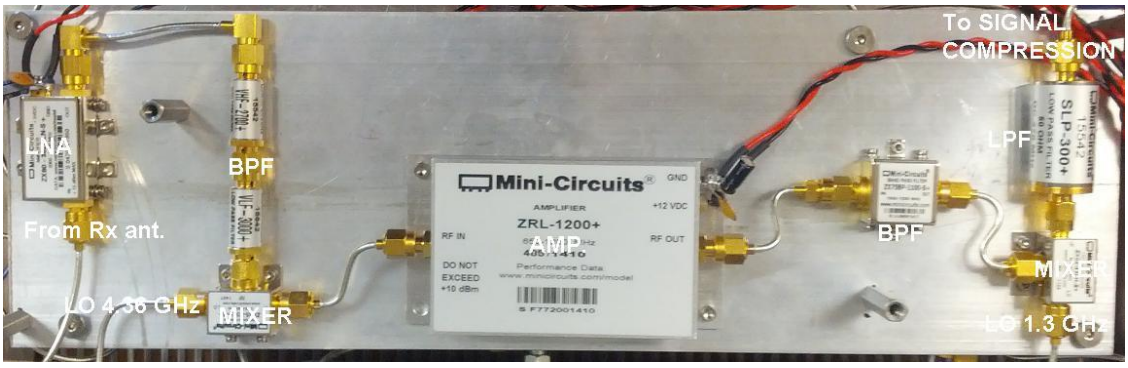

Figure 4.4: **Down-converter. The received signal in the antenna enters the LNA. The pulse is down-converted (travels from the left to the right). Then, it is ready to get compressed.**

4.3 Down-converter

The components used in the down-converter and up-converter are very similar, with the exception of some small differences. Table 4.2 lists the components used in the design. First, the LNA with a NF of 1.05 dB will amplify the pulse received without increasing too much the noise floor. Even if in the specifications the LNA is not working exactly at the desired frequency, its behavior is almost the same. Following the LNA, there are the same filters and mixers used in the up-converter. Moreover, an L-band amplifier and a low pass filter are added. The low pass filter will attenuate all the products that result from the down-conversion and amplification of the signal.

Reference (MiniCircuits)	Component type	Specifications	Use
ZX60-362GLN+	Low Noise Amplifier	Gain 20dB, Noise Figure 1.05dB, P_1=16dBm	Amplifier with low noise figure
VLF-3000+	Low Pass Filter	Passband = DC-3600 MHz	Reject image frequency band
VHF-2700+	High Pass Filter	Passband = 2500-6500 MHz	Clean lower side spectrum
ZX05-83LH+	Mixer	LO Power +10dBm, Conversion Loss 5.6dB	Down-conversion to L-band
ZRL-1200LN+	Amplifier	Gain 26dB, P_1=24dBm	Amplify received pulse at L-band
ZX75BP-1100+	Band Pass Filter	Fast roll-off on the upper side band, Passband=1000-1200 MHz	LO attenuation and image frequency band rejection
ZX05-43LH+	Mixer	LO Power +10dBm, Conversion Loss 6.3 dB	Down-conversion to Base band
SLP-300+	Low Pass Filter	Passband=DC-300MHz	Filtering before pulse compression mixer

Table 4.2: Components used in building the down-converter. All of them have SMA connectors.

4.4 Signal compression

The signal compression stage contains the elements shown in Table 4.3. The high pass filter is supposed to help the DC-block to reject the low frequency signals. It was built in a little FR4 PCB. There are two low pass filters: one after the mixer and another one before the ADC. The first LPF has a cutoff frequency of 5 MHz. The flight plan predicts that, at the highest altitude, the frequency that covers the maximum range is 5 MHz. Thus, to avoid aliasing, the filter must attenuate the frequencies higher than 5 MHz, including the sum of frequencies resulting from the mix operation.

After the amplifiers and before the ADC there is the other LPF. Since the sample frequency used in most of the measurements is 5 MHz, the maximum frequency of the signal cannot be higher than 2.5 MHz if Nyquist sampling theorem wants to be satisfied. The filter will ensure unwanted signals (e.g. intermodulation products of the amplifiers) cannot cause aliasing.

Reference (MiniCircuits)	Component type	Specifications	Use
ZX05-1L+	Mixer	LO Power +3dBm, Conversion Loss 5.7dB	Pulse compression, the output is the beat frequency
High Pass Filter v1	High Pass Filter	Passband > 200 kHz	Reduce the near field coupled energy
SLP-5+	Low Pass Filter	Passband = DC-5MHz	Noise reduction, filter spurious signals
BLK-89+	DC block	Passband > 100 kHz	Reduce the near field coupling
ZFL-500+	Amplifier	Gain 22dB, P_1=10.9dBm	Amplify beat frequency before sampling
BLP-1.9	Low Pass Filter	Passband = DC-2.5MHz	Anti-aliasing filter

Table 4.3: **Components used in building the signal compression stage. All of them have SMA connectors.**

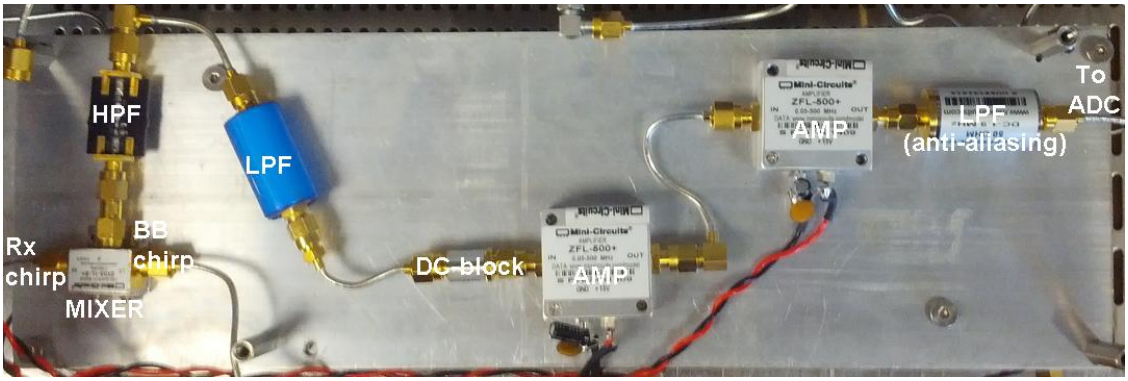

Figure 4.5: **Signal compression. The received chirp comes from the down-converter and it is mixed with the BB chirp (before Tx) to get the beat frequency. After some filters and amplifiers, it is ready to be sampled.**

Reference (MiniCircuits)	Component type	Specifications	Use
ADF4350	Frequency Synthesizer with VCO (Eval. Board)	Band = 137.5 - 4400 MHz	Local oscillator at 1.3GHz and at 4.36GHz.
ZFSC-2-6+	Power Splitter	Insertion Loss 3.3dB	10 MHz reference signal splitting
ZFSC-2-1+	Power Splitter	Insertion Loss 3.3dB	Chirp pulse splitting
ZFSC-2-5+	Power Splitter	Insertion Loss 3.8dB	1.3 GHz splitting
ZX10-2-71+	Power Splitter	Insertion Loss 3.2dB	4.36 GHz splitting
ZX60-2510M	Amplifier	Gain 12.8dB, P_1=16dB	1.3 GHz amplifier
ZX60-V83+	Amplifier	Gain 13dB, P_1=17.5dB	4.36 GHz amplifier

Table 4.4: Components used in building the local oscillators stage. All of them have SMA connectors.

4.5 Local oscillators stage

This stage contains the components listed in Table 4.4. The LOs are prototype boards. They are inexpensive. The LO frequency and the power can be modified easily using the provided software. However, there are disadvantages to using them, such as having to configure them each time the system is turned on, as well as their big dimensions. It is recommended that these disadvantages be taken into account in the future. Two splitters are used to bring the chirp signal to the up-converter and to the two signal compression stages. Two splitters for each LO are also needed to bring their signal to the up-converter and both down-converters.

4.6 Filters

The selection of filters already built that can be found in the market is big. However, it is hard to find the perfect filter that suits exactly a particular system. The best option to get a filter with the desired response is to design it.

For the S-band radar two different types of filters were designed: the coupled lines filter and the symmetric interdigital filter.

- The coupled lines filter is a narrowband bandpass filter. It is made with cascaded half-wavelength coupled line sections. Each line is open circuited at both ends [1, 2].

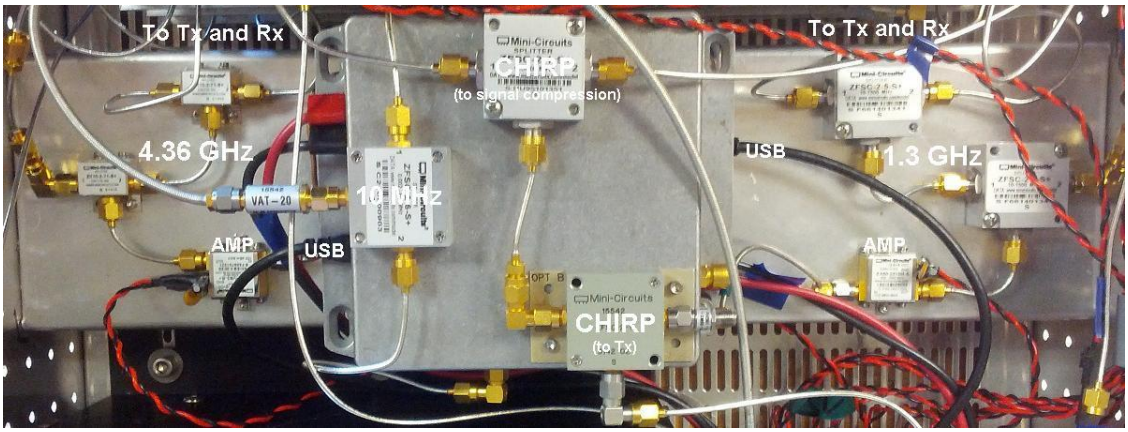

Figure 4.6: **Local oscillators with splitters and amplifiers. The chirp is split to the up-converter and to the signal compression stage.**

- The symmetric interdigital filter is a bandpass filter. It is made of an array of quarter-wavelength line sections. Each line has an open-circuited end and a short-circuited-end [2].

Each type of filter has its pros and cons. The coupled lines filter is easily designed and built. The simulations and the actual response are expected to match easily since they have a simple design. On the other hand, the interdigital filter's design and manufacturing is slightly harder. The need of vias makes more difficult to get a response similar to the simulations because of the manufacturing method used.

However, the interdigital filter has some interesting characteristics that make it worthwhile to build because it is more compact than the coupled line filter, and its size is significantly reduced. Moreover, the second passband of the filter is centered at three times the midband frequency while, in the coupled line filter, the second passband is centered at two times the midband. When the second passband is centered at two times the midband, the image frequency band is near and its rejection is not efficient [2].

The first filters built were coupled lines filters. They were built in FR4 substrate. FR4 is cheap but its specifications at L-band and S-band are nonlinear and hard to predict. The whole design relies on properties like the dielectric constant of the substrate. If the substrate used differs from the one used in the design, the results probably will be far from the simulations. The main problems found were a big shift in frequency and big insertion loss in the passband.

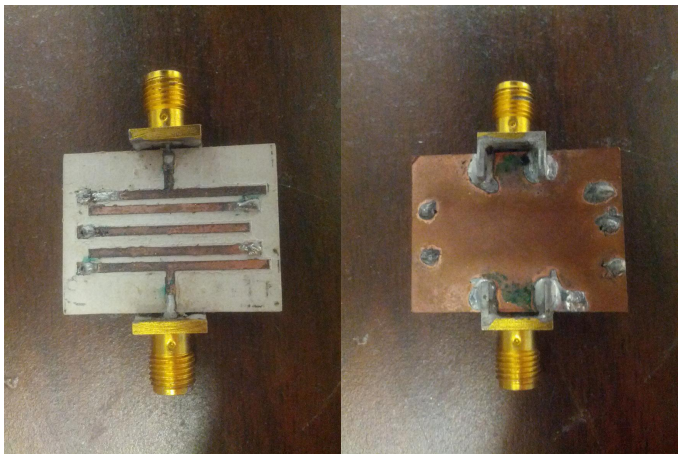

Figure 4.7: L-band symmetric interdigital filter designed and built in the laboratory.

Because of this, RO3010 substrate (from Rogers Corporation) was used instead. Their specifications are known and stable at high frequencies. The results obtained were better than using FR4. However, the milling machine used is not always accurate, resulting in lines shorter than designed or vias without copper on the top layer. Several designs were built to get good results.

Figure 4.7 shows one of the symmetric interdigital filter designed and built. The dimensions (without the SMA connectors) are 2.2 cm x 2.9 cm. The milling machine rubs out the copper and drills the holes for the vias. Then, the SMA connectors need to be soldered. The last step is to fill the via holes with a wire to connect the top layer with the ground plane. The inductance added by the vias is taken in account beforehand when the filter is designed. However, it is hard to use the same amount of solder and wire on each via in different designs. Thus, the inductance is not always the same, and its effect is specially noticeable at S-band. This step is hard to replicate to get similar responses from different manufactured filters that have the same design.

Figure 4.8 shows the response of the symmetric interdigital filter. The insertion loss in the passband has a flat response and its range goes from 0.8 dB to 1 dB. The bandwidth is approximately 225 MHz and the center frequency is 1.16 GHz. The upper cutoff frequency is 1.28 GHz and it is sharp enough to reject the 1.3 GHz local oscillator and the image frequency. The image frequency band would be attenuated more than 40 dB.

The phase response and group delay of the designed filter is shown in Figure 4.9. The group delay shows a flat time response until the upper cutoff gets closer. A different approach to understand the same concept is to check the phase response. As the image shows, the phase

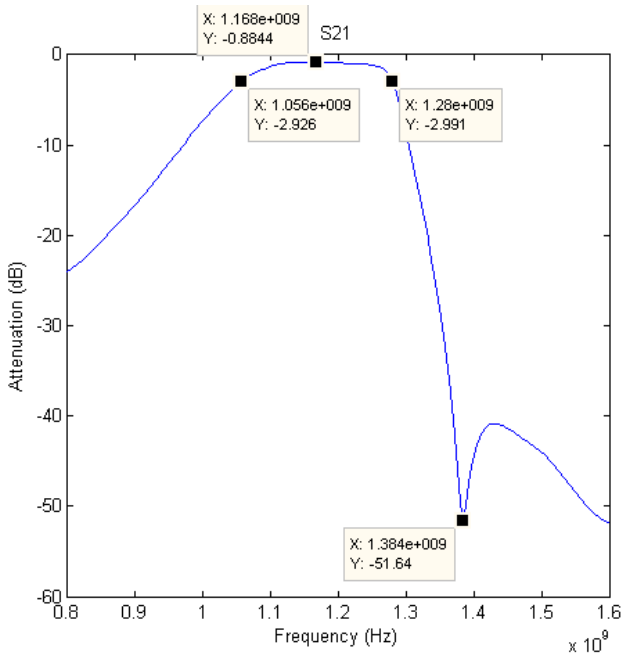

Figure 4.8: Measurement, made with a network analizer, of the magnitude of S21 of the symmetric interdigital filter.

response is linear inside the passband of the filter. In the transition band, between the pass- and stop-bands, there is a sharp phase change in the cutoff frequencies. It can be noticed that, before reaching the upper cutoff frequency defined in Figure 4.8, the phase stops being linear. In the S-band system, it should not be a problem since the band used is in the linear phase band. To maintain a linear phase response, or a flat time delay, is important if interferometry is used.

The filters built in the laboratory were fragile and it was hard to get two filters with the same response. Since the system must work in the aircraft, it is too risky to mount a component that changes its response with vibrations. Furthermore, the receivers must be as symmetric as possible to get the same phase response. In the final design, MiniCircuits filters were used instead because of their robustness and almost identical response between the same filter model.

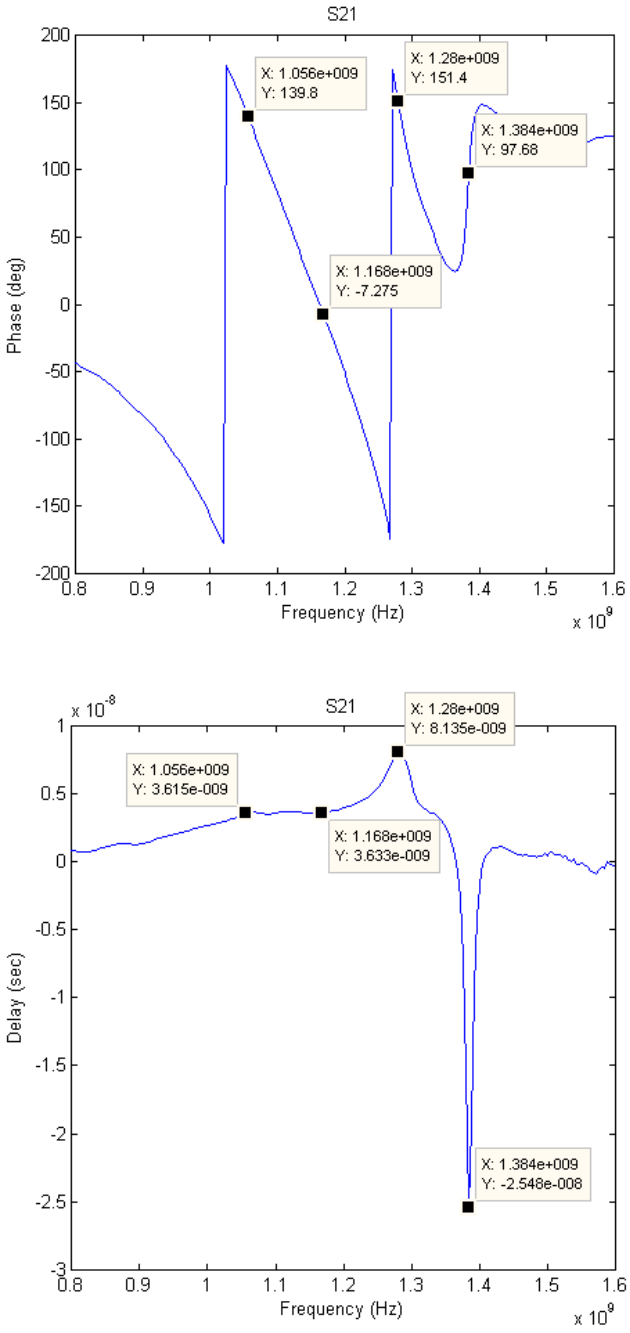

Figure 4.9: **Group delay and phase response of the symmetric interdigital filter measured with a network analizer.**

CHAPTER 5

Ground measurements

Before taking measurements from the airplane, the system was tested from the ground. Since at this stage, the radar is on its initial design, several measurements were done to characterize the system, to decide the appropriate chirp parameters, the position of the antennas and the acquisition configuration.

The initial measurements were taken from the roof of the Lederle Graduate Research Center (LGRC). LGRC is situated on campus and its height is 60m. It gives a privileged view of UMass campus. The look angle from the roof is too high, resulting in a bad SNR. Moreover, the low resolution in azimuth due to the antennas' beamwidth makes it particularly hard to discern individual targets in the radar's look direction. However, the first results were useful to determine that the transceiver was working.

The next step was testing the system at Mount Sugarloaf which will be explained in the following sections.

Figure 5.1: Measurement from LGRC roof at early stages of the radar's development.

Figure 5.2: Google earth view of the area scanned in the ground measurements from Mount Sugarloaf.

5.1 Setup

Mount Sugarloaf has a pavilion offering views of the Connecticut River, Sunderland and Deerfield. The variety of targets (trees, fields, water, buildings, roads and mountains) makes Mount Sugarloaf the perfect place to take measurements before setting up the system on the aircraft.

The measurements were taken pointing to two opposite sides: Sunderland and Deerfield. Sunderland's side gives better results since it offers the view of the river, an easy recognizable feature. Thus, the results presented will focus on this area, showed in Figure 5.2.

The system was mounted in a rack mount: the radar, the power supply, the acquisition computer and the signal generator.

Since the radar is not moving while taking the ground measurements, a positioner is needed to scan the area. The positioner is able to tilt vertically and to rotate horizontally. Therefore, the look angle can be adjusted and the chosen area observed. The antennas are mounted in the positioner.

In some of the measurements, the goal was to create a synthetic array of antennas to improve the resolution. In that case, the antennas were moved horizontally in a straight line by the technician, no positioner was used.

Figure 5.3: Deployment of the system at Mount Sugarloaf.

Figure 5.3 shows the typical setup of the system.

During all the measurements, the main problem that needed to be solved was the coupling between the transmitter and the receivers antennas. Thus, the setup of the antennas was changed several times to find the best spacing and positioning to avoid the coupling.

5.2 Results

This section presents the results of the ground deployments and discuss main issues of the system such as the coupling between the transmitter and the receiver.

The coupling has two different sources. The main source is the near field coupling between the antennas. The second is the coupling through the ground plane.

The coupling between antennas saturates the receiver resulting in a ripple in the spectrum as seen in Figure 5.4. Moreover, the coupling through the ground plane raises the noise level. Because of these effects, the spectrum is not decreasing its power at further range, or higher frequencies. Therefore, the SNR of the system is usually low and small targets are hard to see due to the poor sensibility. Figure 5.5 is a good example of how the power of the spectrum is

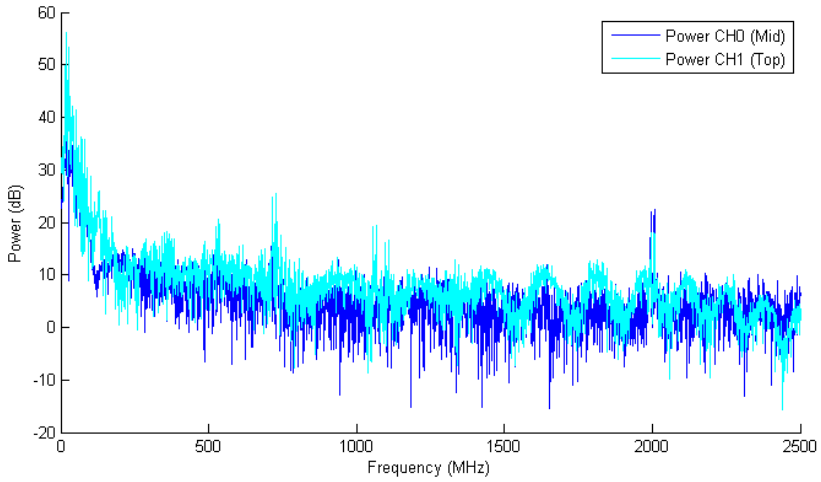

Figure 5.4: **Typical ripple in the spectrum of a ground measurement. CH0 corresponds to the antenna in the middle of the plate (closer to the transmit antenna) and CH1 corresponds to the antenna situated further from the receiver.**

not weaker at higher frequencies. In this measurement, an aluminum plate was installed above the transmitter. The channel closer to the transmitter is clearly influenced by the energy being transmitted even with the plate, while the other channel is slightly improved.

The same effect can be seen in Figure 5.6. While in CH1 some features can be seen, in CH0 they are hard to notice. The algorithm to plot the data compensates the range loss by adding power. It is important to realize that the reflectivity scale is not showing the real reflectivity, some corrections should be done to get a more accurate result. However, this is not a critical parameter at this stage.

Since the spectrum is not decreasing power when range is increased, the range loss compensation results in a power increase with range increase, as seen in the picture (especially for CH0).

In order to reduce the effect of the near field coupling between the antennas, three different approaches to reduce this effect were used: reduce the transmitted power, separate the antennas, and isolate the antennas using a conductor plane between them. Reducing the transmitted power helps, but some weak targets may not be detected anyway since their response will be weaker.

Placing the transmitter antenna as far as possible from the receive antennas is also an effective solution. The transmitted power will remain the same while weaker targets will still be detectable. The downside is the impossibility of spacing the antennas as much as needed because of the

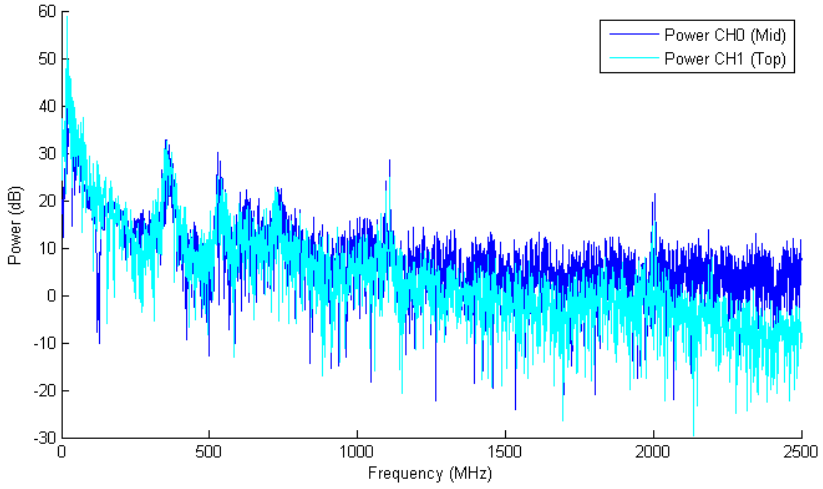

Figure 5.5: **Spectrum of a ground measurement. The response of the same pulse is plotted for each channel. CH1 corresponds to the antenna which is situated farther from the transmitter. An aluminum plate was installed above the transmit antenna.**

limited dimensions of the airplane's door.

Placing a grounded conductor plane between the transmitter antenna and the receiver antennas is a good method of isolation.

An aluminum plate was added above the transmitter. Figure 5.7 shows a measurement using the plate. Both channels have enough sensibility to detect different features. The two lines of trees along the river are easy to recognize. The rest of targets are buildings and trees. The low transverse (azimuth) resolution makes hard to distinguish between them. The transverse resolution in Real Aperture Radar is defined by the equation

$$Res_{az} = range \cdot \theta_H. \tag{5.1}$$

Recall that the antenna azimuth beamwidth (θ_H) is 0.21 rad. For instance, at 1000 m range, the transverse resolution is $Res_{az} = 1000 \cdot 0.21 = 210\,m$. It is easy to notice how it gets worse at further range, for example, in the scan of the river from 50 degrees to 70 degrees. At 50 degrees, the river direction starts to get parallel to the range direction. Therefore, the river trees lines are not in the same range bin anymore. It can clearly be seen how a group of trees result in a wide target, and how these targets get wider and wider at further range.

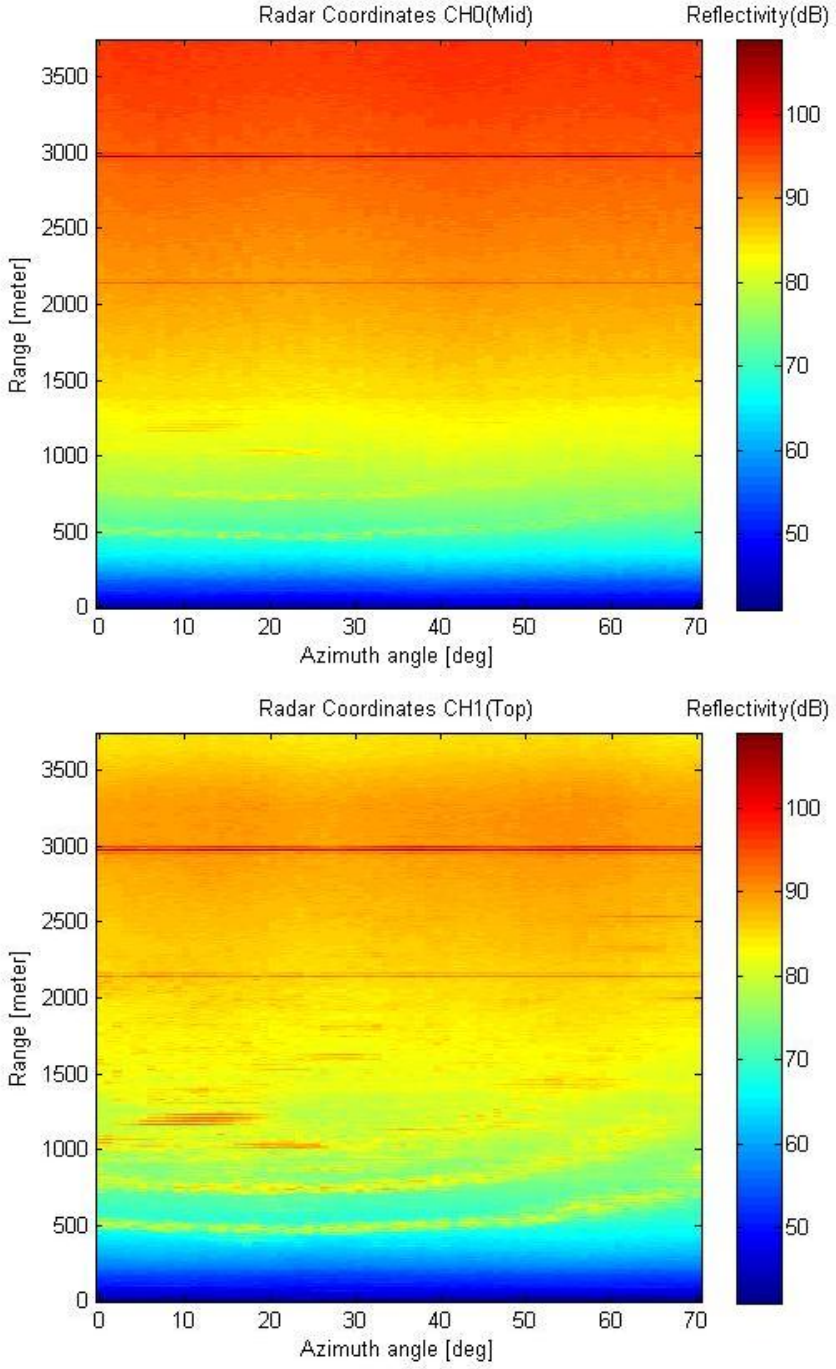

Figure 5.6: Ground measurement. Big near field coupling in CH0 which is closer to the transmit antenna.

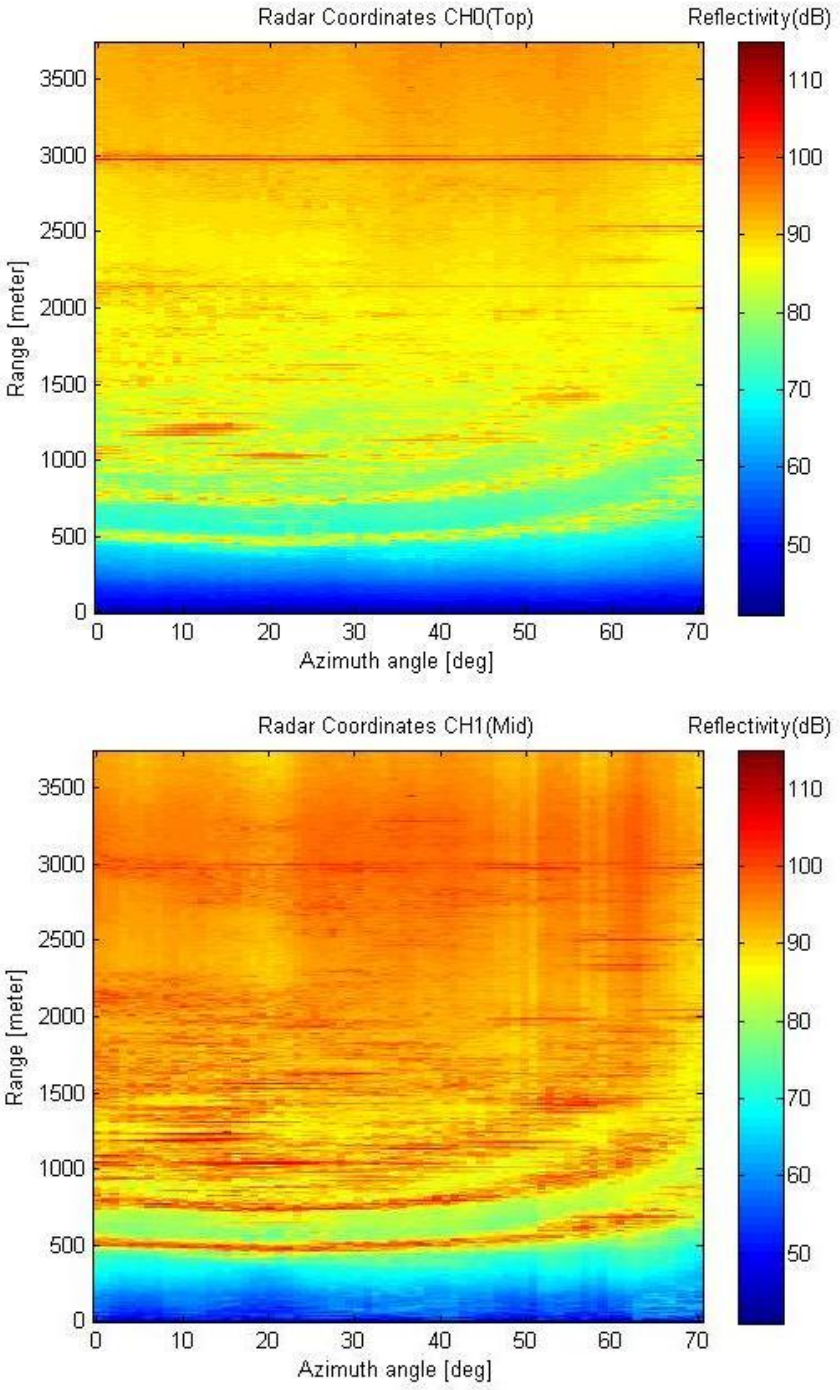

Figure 5.7: **Ground measurement taken from Mount Sugarloaf. A plate was installed above the transmit antenna.**

CHAPTER 6

Flight measurements

Once the results from the ground measurements are repeatable, the next step is to bring the system to the airplane This section will present how the system was installed in an aircraft and the first results gotten from the measurements.

6.1 Setup

At this stage, the system needed to be mounted inside the airplane. To take measurements in the airborne platform, the radar needs its power supply, the acquisition computer, the signal generator, a switch and a laptop. The laptop is connected to the acquisition computer, through the switch, using Windows Remote Desktop. Thus, the acquisition computer is controlled using the laptop.

The airplane is a Cessna 206. The space inside is limited, the system must be mounted properly to leave free space for the technician and the Airborne Imaging Multispectral Sensor (AIMS) system developed at Mount Holyoke [6].

With the S-band radar system, the setup tried to be as close as possible to the one used in TIMMi's deployments. The supporting electronics were mounted in the same 26 x 32 in. plywood board. Since the volume of the supporting electronics is the same, the whole plywood board can be placed vertically in the rear of the aircraft cargo area. The radar box can be placed between the door and the technician's seat and tie it down with straps. The radar should be completely fixed if fitted and strapped down properly. The laptop must be carried by the technician while taking the measurements. The antennas were mounted in the door of the airplane.

Figure 6.1 shows the typical setup of the system.

Figure 6.1: Setup inside the plane.

6.2 Acquisition software and AIMS

The acquisition software used was the LabVIEW code developed by Rockwell B. Schrock[5]. The software supports continuous acquisition while displaying the backscattered power of two channels. It writes the raw RF samples in binary format as well as a timestamp (file version 2). If further information is needed, the reader may refer Rockwell B. Schrock's thesis [5].

The Airborne Imaging Multispectral Sensor (AIMS) is a system developed at Mount Holyoke and it is used for forest research [6]. The system is composed of a LIDAR, a GPS and an Inertial Measurement Unit (IMU). The LIDAR measures the platform height above ground level. However, it could not be used in the measurements since, at the altitude flown, the LIDAR does not work. To get the height, the GPS data was used instead. The IMU gets the pitch, roll and yaw of the platform.

6.3 Flight lines and parameters

Prior to flying, some decisions, like the flight lines or the altitude, need to be made. The flight lines must be chosen so features like the river, trees, fields and buildings can be detected by the radar. The lines chosen are shown in Figure 6.2.

Figure 6.2: **Planned flight lines. The green lines indicate where the lines start, the red lines their end.**

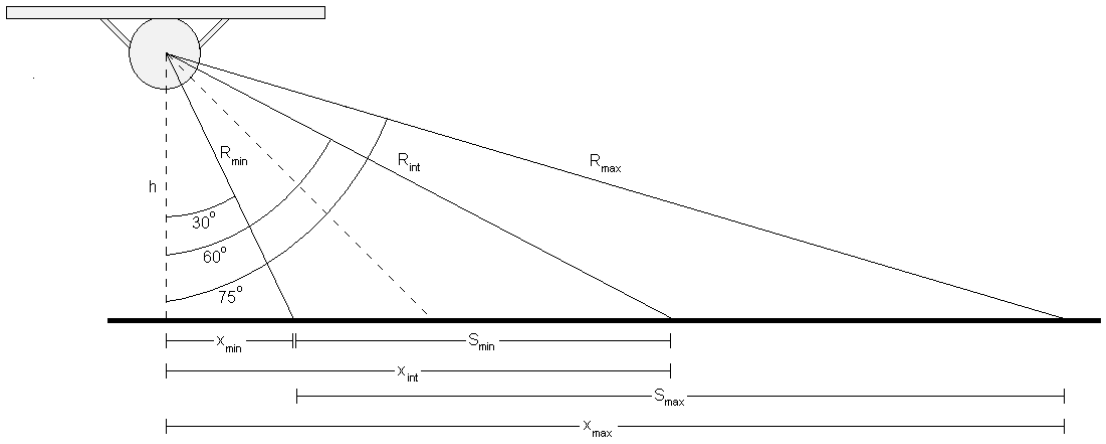

Figure 6.3: Cross-track geometry. The look angle is 45°.

h(m)	$S_{max(m)}$(m)	S_{min}(m)	R_{max}(m)	R_{min}(m)	R_{int}(m)	x_{max}(m)	x_{min}(m)	x_{int}(m)
500	1577	577	1932	577	1000	1866	289	866
1000	3155	1155	3864	1155	2000	3732	577	1732
1500	4732	1732	5796	1732	3000	5598	866	2598
2000	6309	2309	7727	2309	4000	7464	1155	3464

Table 6.1: Swath and range parameters with a look angle of 45°.

The altitude is also an important parameter. It will affect the power received from the ground and the swath will change. Therefore, parameters like the sampling frequency may need a change. Figure 6.3 illustrates the cross-track geometry and Table 6.1 lists the parameters associated at different altitudes. The look angle is 45 degrees. There are two swath defined: maximum swath and minimum swath. The maximum swath is calculated taking in account the extinction of the signal and the beam width. At the maximum swath, the incidence angle of the signal is high and the system sensibility will only allow to detect bright targets, the SNR will be low.

6.4 Initial results

The system was tested once in the airplane. The results obtained from that measurement are presented in this section.

The goal of the flight was to test if the radar was capable of getting good data at different

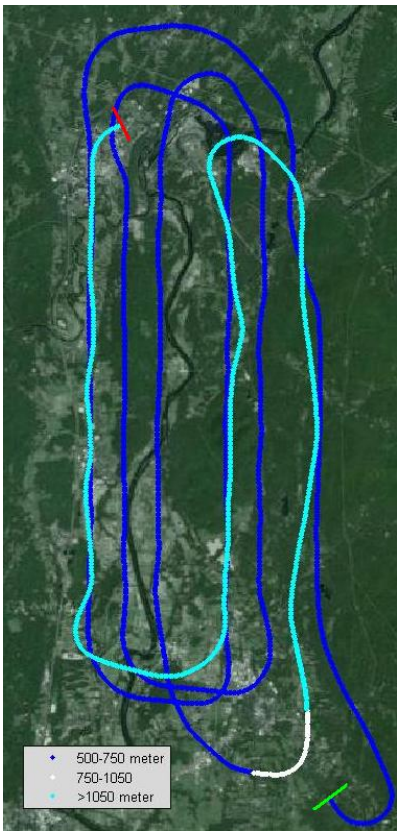

Figure 6.4: Lines flown at two different altitudes: 600 m (blue) and 1200 m (cyan). The green and red lines are the starting and ending points.

altitudes. The flight resulted in an hour and a half of data. There were clouds at two of the altitudes planned (above 1200 m). Thus, the measurements were done at 600 m and 1200 m. Most of the data is taken at 600 m. The flight lines can be seen in Figure 6.4.

The signal generator parameters used in all the flight measurements are listed in Table 6.2. The backscattered power plotted while flying showed good enough results. Thus, in order to have a dataset of continuous data, the same configuration was used during all the flight with just some minor changes between lines. The Voltage peak-to-peak (V_{pp}) was changed several times to get the best sensibility for the far range signals without saturating the ADC too much.

The sample frequency chosen was 5 MHz. The beat frequency equation is $f_b = B \cdot \frac{t_d}{\tau} = \frac{B}{c} \cdot \frac{2r}{\tau}$. The calculated maximum distance, with the maximum frequency 2.5 MHz (Nyquist), is 3750 meter. It is enough when flying at 600 m and almost enough to get the maximum swath when flying at 1200 m.

The data was processed with software written by Kan Fu, a PhD student at MIRSL. In

Function	
Sine	
Run Mode	
Sweep	
Amplitude Menu	
Amplitude	9 dBm
Offset	0 V
Sweep Menu	
Start Frequency	90 MHz
Stop Frequency	190 MHz
Sweep Time	1 ms
Return Time	0 ms
Hold Time	0 ms
Type	Linear
Mode	Repeat
Source	Internal
Slope	Positive
Trigger Interval	1 ms

Table 6.2: Tektronix AFG 3252 function generator flight configuration.

the first results two big problems were noticed:

- The changes made on the antennas' configuration in order to improve isolation between the transmit and receive antennas were not enough to improve the channel closer to the transmitter antenna. Thus, one of the channels had a high noise level that made hard to detect targets resulting in poor images with low SNR.

- The second big problem was the loss of half of the data. The ADC has a re-arming time of 8 μs. Since the chirp pulse is generated continuously, when the trigger of a new pulse is received by the ADC, the re-arming time has not finished yet. The ADC does not receive a trigger to start sampling and saving data until the next pulse starts. Thus, only the data of one pulse every two is sampled and written onto the file. The resulting images are geographically distorted. This distortion can be noticed in the range migration since the hyperbola of each target is steeper than it should be. It can also be observed if distance between targets is calculated and compared to a map of the area.

Figure 6.5 shows some of the images obtained from the flight. They are all from CH0, corresponding to the antenna on the top of the plate. CH1 had the noise floor too high and the SNR

is low.

Different features can be seen in the images: roads, fields, mountains, the river, buildings, power lines... At far range, in the second and third images, it is possible to recognize the pattern made by the ripple in the spectrum. At this range, the look angle is very high, and hence the power of the echo is low. Therefore, only the bright targets raise above the ripple. The swath, 3150 m, is larger than expected. The range migration can be noticed in bright targets. There are some range bins with constant power due to internal interferences of the system. Due to the motion of the aircraft, there are several blurred looks.

At the time of writing, SAR processing techniques have been applied without good results. Because of this and the bad quality of CH1, interferometric images have not been generated.

The images generated with the data obtained in the first flight cannot be used to study the response of natural targets. The whole system must be improved and SAR processing techniques should be used. However, these images prove the radar is capable of getting data in an airborne platform.

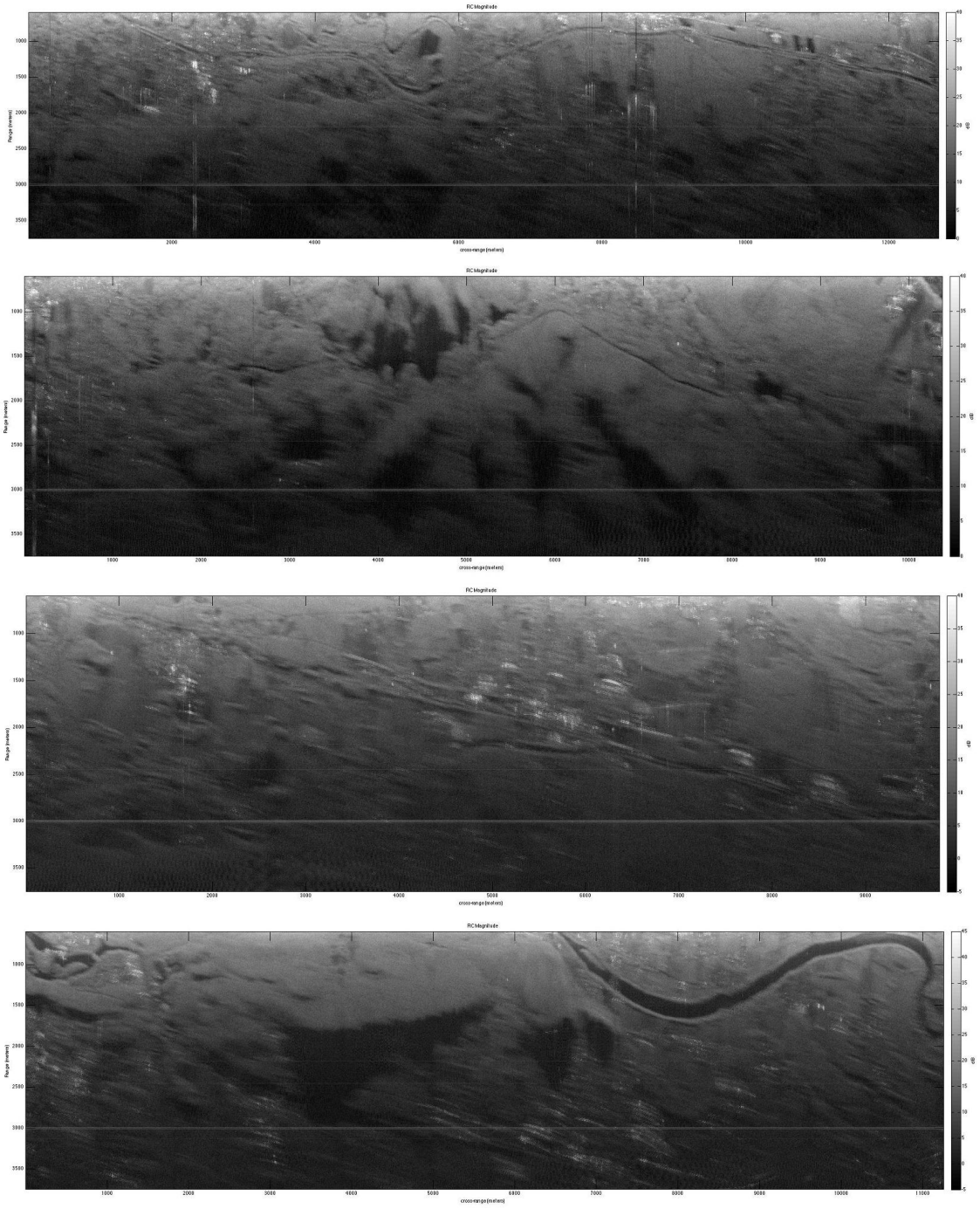

Figure 6.5: **First flight measurements results. The altitude is 600 m. The polarization is vertical. The range scale starts at 600 m and ends at 3750 m. The cross-range varies from 10 km up to 13 km, depending on the image. The dynamic range for the reflectivity scale is 40-50 dB, depending on the image.**

CHAPTER 7

Contributions and future work

7.1 Contributions

Developing the system and bringing it to an airplane required a process of designing, building and testing that lasted several months. The following list describes briefly what it has been developed to complete this thesis:

- Designed and built the whole radar: up-converter, down-converter, signal compression stage, LOs stage.
- Built the radar with all its stages on an aluminum enclosure. This required mounting the components into aluminum plates, wiring the whole system and placing the different stages inside the enclosure.
- Designed and built several microstrip L-band and S-band bandpass filters and a pair of high pass filters.
- Modified an existing power supply enclosure adding new power supplies to adapt it to the S-band system.
- Designed a new mechanical system to attach the S-band antennas to the airplane's door.
- Implemented minor changes on the acquisition LabVIEW existing codes to support new functions like the tilting of the positioner.
- Written basic MATLAB codes to plot the data acquired in the ground measurements.
- Made several ground deployments of the system at different stages of development.
- Diagnosed and improved issues like the saturation of the receiver.

- Planned and adapted the system for aircraft deployments.
- Completed one aircraft deployment and analyzed the data obtained: motion data and the radar data.

7.2 Future work

The radar system presented in this thesis is on its very first stage of development. Thus, the system must be improved in several ways if useful data wants to be acquired:

- The system size and weight must be reduced. If more airplane deployments are planned, a smaller radar enclosure as well as smaller supporting electronics would be recommendable. At the time of writing, the system is too big to leave free space to mount other systems in the plane. There are several changes that can be made to reduce the size:
  - Removing the down-converter and building a new signal compression stage (if FMCW will be used).
  - Finding new LOs.
  - Designing and building the PCB of the transceiver.
  - Finding a smaller HPA.
  - Finding a new ADC.
- The noise level should be reduced. The ground planes of the transmitter (high power signals) and the receiver (weak signals) should be separated and connected by a high impedance point. At the time of writing, all the signals share the same ground plane: all the components are grounded to the enclosure through their own conductor enclosure. Since all the materials used are conductors, it is hard to isolate properly the transmitter and receiver. The design of a PCB, instead of redesigning the actual transceiver in SMA-components, may help to resolve this issue.
- The near field coupling of the antennas should be reduced to improve the whole system behavior. New aluminum plates or microwave absorbers between antennas can be used. Changing the design of the antennas may help too.

- New antennas would be useful to improve different characteristics such as:
  - Transversal (azimuth) resolution. The only way to improve the resolution with the existing antennas is via SAR processing techniques. Narrowing the beamwidth in azimuth would improve the azimuth resolution.
  - Near field coupling. Reducing the beamwidth of the main lobe and reducing the side-lobes would increase the isolation between transmitter and receiver.
  - Increased transmitted chirp bandwidth to improve the range resolution. The system is designed to work with a 200 MHz chirp signal. However, the antennas have 100 MHz bandwidth.
- New door structure with more freedom to point the antennas at different look angles.
- New ground and flight measurements should be done.
- SAR processing.

BIBLIOGRAPHY

[1] David M. Pozar. *Microwave Engineering*. 3rd edition edition. 3.10, 3.10, 3.10, 4.6

[2] Jia-Sheng Hong and M.J. Lancaster. *Microstrip filters for RF/Microwave applications*. 4.6

[3] NASA-ISRO. The NASA-ISRO SAR (NISAR) mission concept. 1.1

[4] NASA JPL. NASA-ISRO SAR mission (NISAR). 1.1

[5] Rockwell B. Schrock. *Integration and measurements of a Ka-Band interferometric radar in an airborne platform*. Master's thesis, University of Massachusetts Amherst, 2012. 3.1, 6.2

[6] Thomas L. Millete and Christopher D.Hayward. Detailed forest stand metrics taken from AIMS-1 sensor data. 6.1, 6.2

APPENDIX A

Notation Reference

A.1 Symbolic Notation

B	Bandwidth (Hz)	N_o	Output noise power (dBm)
c	Speed of light in free space ($3 \cdot 10^8$ m/s)	r	Range (m)
τ	Chirp/pulse length (s)	θ_H	Azimuthal antenna beamwidth (degree or rad)
f_b	Beat frequency (Hz)	θ_V	Elevation antenna beamwidth (degree or rad)
IP_3	Third-Order Intercept Point (dBm)	V_{pp}	Peak-to-peak voltage (V)

A.2 Abbreviations

AC	Alternating Current	JPL	Jet Propulsion Laboratory
ADC	Analog to Digital Converter	LNA	Low Noise Amplifier
AFG	Arbitrary Function Generator	LO	Local Oscillator
AIMS	Airborne Imaging Multispectral Sensor	NASA	Nation Aeronautics and Space Administration
BB	Baseband	NF	Noise Figure
DC	Direct Current	NI	National Instruments
FMCW	Frequency-Modulated, Continuous-Wave	NISAR	NASA-ISRO Synthetic Aperture Radar
GND	Ground	RAR	Real Aperture Radar
HPA	High Power Amplifier	SAR	Synthetic Aperture Radar
IMU	Inertial Measurement Unit	SLL	Side Lobe Level
ISRO	Indian Space Research Organization	SNR	Signal to Noise Ratio
		TIMMi	Topographic Ice Mapping Mission